International Journal of Science Academic Research
Vol. 05, Issue 12, pp.8728-8736, December, 2024
Available online at http://www.scienceijsar.com

ISSN: 2582-6425

Research Article

REMOVAL OF A BASIC ORGANIC DYE METHYLENE BLUE FROM AQUEOUS SOLUTION BY ADSORPTION ONTO A LOW-COST BIOSORBENT MADE FROM WATER HYACINTH (*EICHHORNIA CRASSIPES*)

***Anatole KIA MAYEKO KIFUANI, LESALYA MBENGE, Kifline MILEBUDI KIFUANI, Bernick WEMBOLOWA TSHENE and Marie Zola Tuluenga**

Laboratory of Physical Organic Chemistry, Water and Environment, Department of Chemistry and Industry, Faculty of Sciences and Technology, University of Kinshasa, P.O. Box 190 Kinshasa XI, Democratic Republic of Congo

Received 18th October 2024; **Accepted** 14th November 2024; **Published online** 16th December 2024

Abstract

The aim of this study was to evaluate the ability of water hyacinth (*Eichhornia crassipes)* used as biosorbent (ECB) to remove methylene blue dye (MB) from water. Adsorption was carried out in batch tests by varying several parameters including mass of the biosorbent, contact time, initial concentration and pH of the MB solution. After adsorption the supernatant was analysed by UV-Visspectrophotometry to determine the residual concentration of the MB solution. Adsorption modeling was done with the surface reaction kinetic model and Langmuir and Freundlich equilibrium models. The obtained results showed that the biosorbent from water hyacinth ECB has apH_{ZPC} of 5.51, a specific surface area of 292.52 m^2 g^{-1} and a maximum observed capacity (Q_{mo}) of 89.99 mg g^{-1}. The maximum adsorption percentage increases with biosorbent mass, contact time, and initial MB concentration due to the availability of the number of active sites that gradually saturate to reach the maximum apparent adsorption percentage ($\%_m Ads$) and the maximum apparent adsorption capacity (Q_m).The maximum adsorption capacity and maximum adsorption percentage increase with the pH of the solution due to stronger electrostatic interactions appearing at pH above the pH_{ZPC} between ECB surface and cationic ions from MB.The optimal adsorption weight was evaluated to be 800 mg, with a $\%_m Ads$ of 88.63% at pH 8.06, after 270 min. The modeling results show that adsorption of MB on ECB is best described by the pseudo-second-order kinetic model and the Langmuir model. The values of R_L and $1/n$ lower than 1 indicate that the adsorption of BM on ECB biosorbent is favorable. Thus, water hyacinth biosorbent is promising for the biosorption of methylene blue dye from wastewater.

Keywords: *Eichhornia crassipes*, Methylene blue, Adsorption, Biosorbent, Kinetic, Isotherm.

INTRODUCTION

Water hyacinth (*Eichhornia crassipes)*is a very invasive plant species from Pontederiaceae family. It smothers native vegetation and poses problems of animal and plant biodiversity in rivers and lakes. It reduces insolation and the oxygen content of waterways and leads to eutrophication. The transformation of water jacinth into a biosorbent is a way of recovering it and cleaning up water polluted by organic dyes.

Organic dyes are used in several applications including the dyeing of textiles, cotton, paper. wood and silk.When used, approximately 15 to 25% of organic dyes are released into wastewater effluent without prior treatment. They thus pollute waterways because of their toxicity and persistence in the environment (Jan *et al.,* 2022). Ali *et al.* (2021), Thiene *et al.* (2024) reported that the majority of organic dyes are persistent, refractory and toxic for animal species and humans. Methylene blue is one of the dyes widely used in the textile industry (Pathiana *et al.,* 2017; Jia *et al.,* 2018). It can inductive various diseases by contact, inhalation or ingestion, including burning sensations in the mouth, nausea, vomiting, diarrhea, gastroenteritis, perspiration, cold sweats, permanent injury to the eyes of humans and animals. The treatment of wastewater loaded with organic dyes therefore becomes imperative for the environmental and human safety (Le *et al.,* 2021; Nyakairu *et al.,* 2024).

Corresponding Author:** ***Anatole KIA MAYEKO KIFUANI,
Laboratory of Physical Organic Chemistry, Water and Environment, Department of Chemistry and Industry, Faculty of Sciences and Technology, University of Kinshasa, P.O. Box 190 Kinshasa XI, Democratic Republic of Congo.

The elimination of organic dyes from water is carried out using several methods classified into biological, chemical and physical methods, including a variety of techniques such as: adsorption, advanced oxidation, biosorption, chemical and electrochemical oxidation, coagulation, filtration, flocculation, Fenton electron process, microbial and fungal decolorization, photocatalysis, nanofiltration, ozonation, reverse osmosis (Vanessa *et al.,* 2017; Kifuani *et al.,* 2018b; Mekky *et al.,* 2020; Basma *et al.,* 2023; Raiyyaan *et al.,* 2024). Rahimian and Zarinabadi (2020), Nadew *et al.* (2023), reported that many of these techniques have proven to be expensive or responsible for the pollution induced from their degradation derivates. Razia *et al.* (2022) reported that of all these methods, adsorption was found to be effective in removing organic dyes from wastewater and activated carbon being the most effective adsorbent; but the high cost of its production and difficult regeneration make it less accessible. Currently, agricultural wastes are used as biomaterials to evaluate their performance in removing organic dyes or metallic trace elements from water. This biomass includes waste from rattan sawdust, apricot stones, banana pith, coconut coir dust, cotton stalk, hazelnut shell, coffee residue, coir pith stone, green pea peels, groundnut shells, mango leaves, mango seed kernel, oil palm shell, orange peel, peach stones, sugarcane bagasse, sunflower stalks, yellow passion fruit waste, *Curcumeropsis manni* shells, *Hevea brasilliensis* seed coat, *Manihot esculanta* kernels. These materials contain organic substances such as polyphenols, lignin, tannins, pigments and protein which provide surface functions, such as carboxylic acid, ketone, aldehyde, phenol, lactone, pyrone, responsible for the adsorption of organic compounds or other pollutants on their

surface (Pathiana *et al.,* 2017; Jia *et al.,* 2018; Kifuani *et al.* 2818a; Mobolaji *et al.,* 2021; Hatiya *et al.,* 2022; Imram *et al.,* 2022; Basma *et al.,* 2023 ; Gani *et al.,* 2023 ; Thiene *et al.,* 2024). The aim of this study is to evaluate the effectiveness of the biosorbent based on water hyacinth in the adsorption of methylene blue from water. The effects of different adsorption parameters were studied including dose of adsorbent, contact time, initial concentration and pH of methylene blue solution.

MATERIELS AND METHODS

Adsorbent preparation

The biosorbent was prepared from the stems and leaves of water hyacinth *(Eichhornia crassipes*) collected from the Congo river in Kinkole, Kinshasa, Democratic Republic of Congo. The biomass was firstdried in the sun and then in an oven at 105°C (DESPATCH Oven Co, type Elect)to eliminate of the water content. It was then crushed and sifted to obtain powder with a particle size ≤500 µm. The *Eichhornia crassipes* biosorbent (ECB)thus obtained was stored in airtight packaging and placed in a desiccator at laboratory temperature (28°C), to keep it free from moisture contact and oxidation (Kifuani *et al.,* 2018a).

Adsorbent characterization

The characterization of the biosorbent was done by determining physicochemical parameters including Grain diameter, Humidity, Dry matter, Ash content, pH of zero point of charge (pH_{ZPC}), Specific surface area (S_{MB}) and maximum observed capacity (Q_{mo}).

Grain diameter

The diameter of the grains was determined by sifting using a sieve.

Humidity and dry matter

Humidity (H) and dry matter (DM) were determined by volatilization gravimetry using 5 g of biosorbent ECB, heated in an oven. The water content of the biosorbent (%H) is given by equation 1(Ajala *et al.,* 2024):

$$\%H = \frac{(m_1 - m_2) \cdot 100}{m_1} \quad [1]$$

Where, m_1 and m_2, the weights of biosorbent before and after steaming, respectively.

The dry matter level (%DM) is calculated after deduction of the water content from 100% of the initial sample.

Ash content

For the determination of ash content, 5 g of sample were calcined in a muffle furnace at 600°C (NABER, Model N7/H) for 8 hours to obtain the ash. The ash content (%*A*) of the biosorbent was determined using the following equation 2 (Basma *et al.,* 2024):

$$\%A = \frac{(m_3 - m_4) \cdot 100}{m_3} \quad [2]$$

Where, m_3 and m_4 being the weights of biosorbent before and after calcination, respectively.

Determination of pH_{ZPC}

The pH_{ZPC} (pH of zero point of charge) was determined by the pH drift method. For this purpose, 100 mL of 0.01 mol L^{-1} NaCl solutions are placed in different Adsorbers (LACOPE ADX) and the pH of these solutions is adjusted from 2to 12, by addition of 0.1 N HCl or 0.1 N NaOH solutions, to adjust the acidic or basic solutions, respectively. 1000 mg of biosorbent were then added to each solution and the suspension was stirred for 72 h and centrifuged at 3000 rpm (Centrifuge Labofuge 200 Heraeus). The final pH of each solution was determined using a pH-meter (Hanna Instruments). The point of intersection of the curve obtained by plotting the final pH as a function of the initial pH of each solution determines the pH_{ZPC} (Kifuani *et al.,* 2012; Musah *et al.,* 2020).

Determination of the maximum observed capacity (Q_{mo}) and specific surface area (S_{MB})

The specific surface area of the biosorbent was determined by adsorption of methylene blue using the Kifuani volume variation method (KVVM).This method consists of studying adsorption of methylene blue, at equilibrium time, using a low mass of adsorbent. To 5 mg of adsorbent, increasing volumes (100 mL to 1000 mL) of the MB solution 50 mg/L are added. The suspension is stirred at the equilibrium time previously determined experimentally. The determination of the residual concentration of the supernatant by UV-spectrophotometry makes it possible to calculate the maximum adsorption capacity (Q_m) and the maximum adsorption capacity ($\%_m Ads$), using equations 3to 5. The curve obtained by plotting the maximum adsorption capacity (Q_m) as a function of the volume (V) of the MB solution makes it possible to determine the true maximum adsorption capacity, which we call maximum observed adsorption capacity(Q_{mo}), the others being apparent maximum capacities (Q_m). The maximum observed adsorption capacity is given by the plateau of this curve (Kifuani *et al.,* 2012; Kifuani, 2013; Kifuani *et al.,* 2018a).

$$A = \varepsilon . l . C \quad [3]$$

With, A being the absorbance, ε the molar absorption coefficient (L mg^{-1} cm^{-1}), l the thickness of the cell (1 cm) and C, the concentration of the solute (mg L^{-1}).

$$Q_m = \frac{(C_o - C_e)V}{m_B} \quad [4]$$

$$\%_m Ads = \frac{C_o - C_e}{C_o} \times 100 \quad [5]$$

With, Q_m being the maximum adsorption capacity of the biosorbent (mg g^{-1}), C_o the initial concentration of methylene blue solution (mg L^{-1}), C_e the residual or equilibrium concentration (mg L^{-1}), V the volume of the methylene blue solution (L) and $\%_m Ads$, the maximum observed adsorption percentage.

The specific surface area (S_{MB}) is then calculated according to the following equation 6 (Kifuani *et al.,* 2012):

$$S_{MB} = Q_{mo} . N_A . s \quad [6]$$

Where, S_{MB} being the specific surface area determined using MB as adsorbate (m^2 g^{-1}), Q_{mo} the maximum observed adsorption capacity (mg g^{-1}), N_A the Avogadro number (6.022 10^{23} mol^{-1}) and *s*, the area occupied by a MB molecule (175 $Å^2$).

Adsorbate and adsorbate solutions

Methylene blue, a cationic thiazine dye, was used in this study as a model of organic dye and also it is recommended for the characterization of adsorbents. His IUPAC name is 3,7- Bis (dimethylamino) phenothiazin- 5- ium chloride. Its chemical formula is $C_{16}H_{18}N_3SCl$ and Mw 319.852 g mol^{-1}. It has a flat surface of 175 $Å^2$. Methylene blue used in this study was obtained from Merck and used without purification. All the reagents used in this study were of analytical grade. The chemical structure of MB is given by Figure 1.

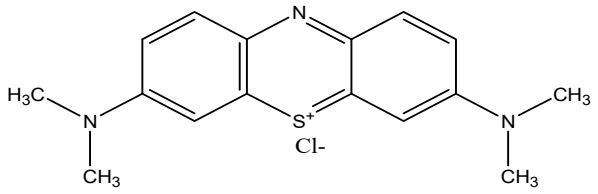

Figure1. Structure of Methylene Bleu

Methylene blue solutions were prepared by dissolving MB crystals in distilled water and diluting the resulting solution to obtain solutions ranging from 1 mg L^{-1} to 100 mg L^{-1}. The pH of the MB solutions was adjusted by adding 0.1 N HCl or 0.1 N NaOH solutions to obtain solutions ranging from pH 2 to 12. The MB solutions, before and after adsorption, were analyzed using a UV-Vis spectrophotometer (HACK Spectrophotometer, SP, model 1105) at maximum length wave for each pH. The Beer-Lambert equation (equation 3)was used to calculate the residual concentration of the MB solution (Raiyyaan *et al.,* 2021).

Batch adsorption experiments

The adsorption tests were carried out in batch experiment with adsorbers (LACOPE ADS) by varying the following parameters: the mass of the biosorbent (1mg-1000mg), the concentration(1 mg L^{-1} to 100 mg L^{-1}) and pH(2-12) of the MB solution and the contact time (0-400 minutes). Before use, the ECB biosorbent was dried in an oven at 105°C for 3 h and the mass of the biosorbent was determined by weighting using an analytical balance (HEB-E 303). The adsorption tests were carried out with 100 mL of MB solution and the required mass of biosorbent. After stirring for the required time, the suspension was centrifuged at 3000 rpm for 30 minutes and the supernatant was analyzed with a UV-Vis spectrophotometer at the appropriate wavelength, to determine the residual concentration of MB solution. Each experiment is repeated three times to determine the absolute error. The adsorption capacity (Q_e) and adsorption percentage (%*Ads*) were calculated using equations 7 and 8 (Mobalaji *et al.,* 2021):

$$Q_e = \frac{(C_o - C_e)V}{m_B} \quad [7]$$

$$\%\,Ads = \frac{C_o - C_e}{C_o} \times 100 \quad [8]$$

With, Q_e being the apparent adsorption capacity or the equilibrium capacity of the biosorbent (mg g^{-1}), C_o the initial concentration of methylene blue solution (mg L^{-1}), C_e the residual or equilibrium concentration (mg L^{-1}), *V* the volume of the methylene blue solution (L) and %*Ads*, the adsorption percentage.

Adsorption kinetics

The modeling of the adsorption kinetic was done according to Lagergren kinetic model (Mekky *et al.,* 2020; Saad *et al.,* 2024) using the kinetic equations of the surface reaction of pseudo-first-order and pseudo-second-order developed by Kifuani (Kifuani *et al.,* 2012; Kifuani, 2013):

Kifuani Pseudo-first- order kinetic model:

$$\ell n \frac{q_e}{(q_e - q_t)} = k_1 t \quad [9]$$

With, q_e being adsorption capacity at equilibrium (mg g^{-1}), q_t adsorption capacity at time *t* (mg g^{-1}), q_e-q_t adsorption capacity of free sites, *t* the time (s) and k_1, the constant rate of pseudo-first-order reaction (min^{-1}). The plot of $\ell n \frac{q_e}{(q_e - q_t)}$ versus *t* gives a line whose slope corresponds to k_1, the rate constant of pseudo-first-order reaction.

Kifuani Pseudo-second-order kinetic model:

$$\frac{q_t}{q_e(q_e - q_t)} = k_2 t \quad [10]$$

Where, k_2 is the rate constant of the pseudo- second- order reaction (g mg^{-1} min^{-1}). The plot of $\frac{q_t}{q_e(q_e - q_t)}$ versus *t*, gives a line whose slope corresponds to k_2, the rate constant of the pseudo-second–order reaction.

Adsorption isotherms

The modeling of the adsorption equilibrium was done using the Langmuir and Freundlich models given by the following equations11, 12 and 13 (Alouani *et al.,* 2018; Mekhalef *et al.,* 2018):

Langmuir model:

$$\frac{1}{Q_e} = \frac{1}{Q_m} + \frac{1}{Q_m K_L} \cdot \frac{1}{C_e} \quad [11]$$

Where, Q_e is the apparent adsorption capacity of the biosorbent (mg g^{-1}), Q_m the adsorption capacity at saturation or maximum adsorption capacity (mg g^{-1}), K_L equilibrium constant adsorption (L mg^{-1}) and *C*e, equilibrium concentration. The plot of $1/Q_e$ versus $1/C_e$ gives a line which allows to determine Q_m and K_L, from the intercept and slope, respectively.

The Langmuir separation parameter (R_L) was calculated using equation 12 (Gajendiran *et al.,* 2024; Hajir *et al.,* 2024) :

$$R_L = \frac{1}{1 + K_L C_o} \quad [12]$$

With, K_L being the Langmuir constant (L mg^{-1}) and C_o the initial dye concentration.

Freundlich model:

$$\text{Log } Q_e = \log K_F + \frac{1}{n} \log C_e \quad [13]$$

Where,Q_e the adsorption capacity at equilibrium (mg g^{-1}), K_F the adsorption constant (Freundlich constant), C_e the concentration of the adsorbate at equilibrium (mg L^{-1}) and n, the Freundlich constant, characterizing the affinity of solute for the adsorbent (affinity parameter). The plot of log Q_e versus log C_e gives a line which allows to determine K_F and $1/n$ from the intercept and slope, respectively.

RESULTS

Characteristics of the biosorbent ECB

The physicochemical characteristics of ECB biosorbent are given by Table 1.These results show that the specific surface area of the biosorbent is 296.52m^2 g^{-1}witha maximum observed adsorption capacity (Q_{mo}) of 89.99 mg/g. The biosorbent is weakly acidic and has a pH_{ZPC} of 5.51.

Tableau 1. Physicochemical parameters of ECB

Parameters	Values
Particulesize(µm)	≤500
Ash(%)	4.40
Humidity(%)	5.38
Drymatter(%)	94.62
pH_{ZPC}	5.51
Q_{mo}(mgg^{-1})	89.99
S_{MB}(m^2g^{-1})	296.52

Effect of biosorbent amount

The effect of the amount of biosorbent on adsorption of MB on ECBis given by Table 2, Figures 2 and 3.The results obtained show that the maximum adsorption capacity of ECB decrease from 30.56mg/g to 4.33mg/g when the amount of the biosorbent increases from 100g to 1000 g(Table 2, Figure 2). In the other hand, the maximum adsorption capacity increases from61.13%to86.63%, when the mass of the biosorbent increase (Table 2, Figure 3).The optimal adsorption weight was evaluated to be 800 mg, with a %m*Ads* of 86.13% and Q_m of 5.38 mg/g, after 210 min. After this amount of biosorbent, the maximum adsorption capacity and the maximum adsorption percentage tend towards constants.

Table 2. Maximum adsorption capacity (Q_m), maximum percentage of adsorption ($\%_m$*Ads*) and equilibrium time (t_e) at different weights of biosorban t(m_{ECB})

m_{ECB}(mg)	Q_m(mgg^{-1})	$\%_m$*Ads*.	*t*.e(min)
100	30.56	61.13	300
200	17.63	70.50	300
400	9.70	77.63	270
600	6.64	79.63	240
800	5.38	86.13	210
1000	4.33	86.63	190

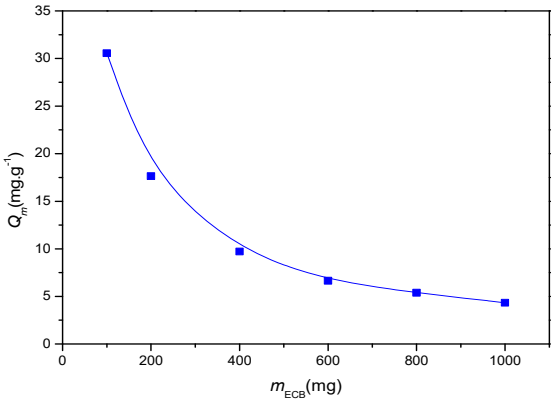

Figure 2. Maximum adsorption capacity (Qm) vs dose of biosorbent (mECB)

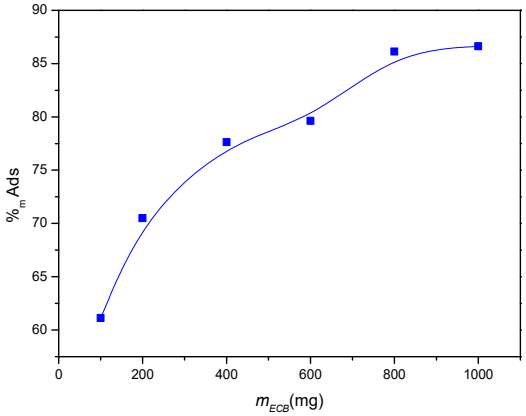

Figure 3. Maximum percentage of adsorption ($\%_m$Ads) vsdose of biosorbent (mg)

Effect of contact time

The results on the effect of contact time between ECB-MB are presented in Figures 4 to 9 for different mass of adsorbent, different initial concentration and pH of methylene blue solutions. From these results it appears that the adsorption capacity and the adsorption percentage of the biosorbent increase with ECB-MB contact time. The optimum equilibrium time is estimated at 300 minutes for all parameters. The curves obtained by plotting the adsorption capacity or the adsorption percentage vs ECB-MB contact time show three adsorption phases: a first rapid phase at the start of adsorption, followed by a second slow phase and a third adsorption phase during which adsorption is constant.

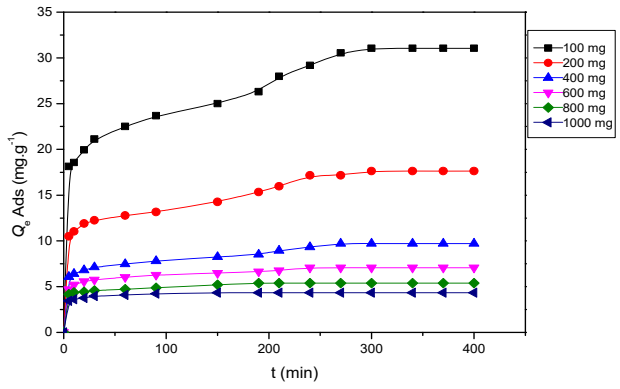

Figure 4. Effect of contact time on adsorption capacity (Q_e) of ECB at different doses of biosorbent

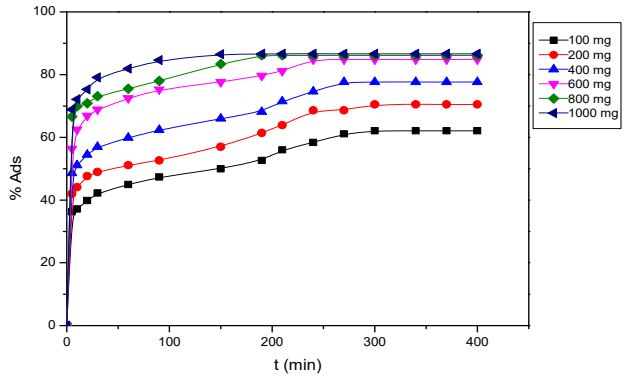

Figure 5. Effect of contact time on the percentage of MB adsorption on ECB at different doses of adsorbent

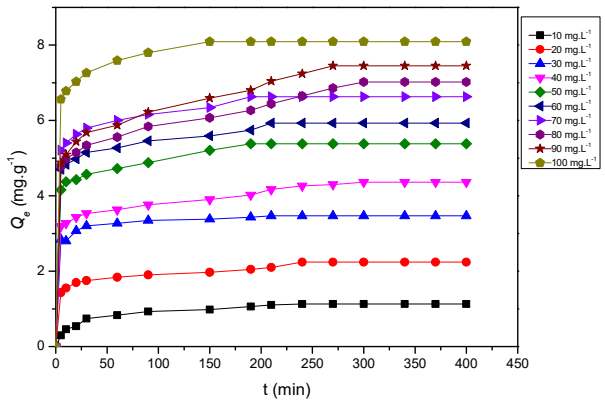

Figure 6. Effect of contact time on the adsorption capacity of ECB at different initial concent rations of MB

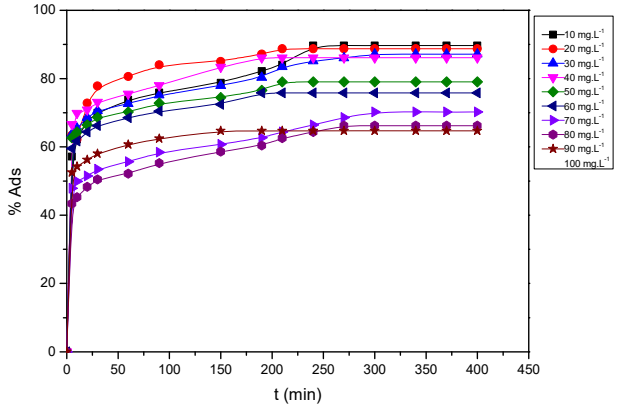

Figure 7. Effect of contact time on the percent age of adsorption of ECB at different initial concent rations of MB

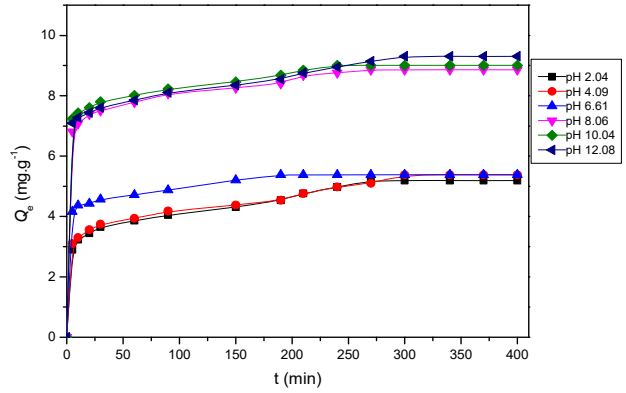

Figure 8. Effect of contact time on the adsorption capacity of ECB at different pH

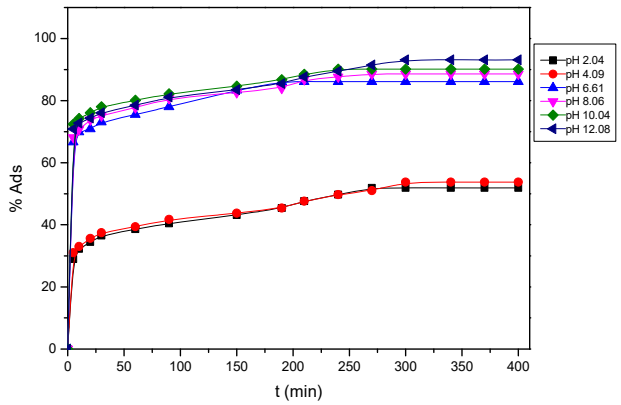

Figure 9. Effect of contact time on the percentage adsorption of ECB at different pH

Effect of initial Methylene blue concentration

The effect of the initial concentration of MB on the adsorption is given by Figures 10 and 11.Figure 10 shows an increase in the maximum adsorption capacity from 1.13 mg/g to 8.02 mg/g when the initial concentration of the MB solution increases, whereas Figure 11 shows a decrease in the maximum adsorption percentage from 90.63% to 64.69% with the increase in the initial concentration of MB.

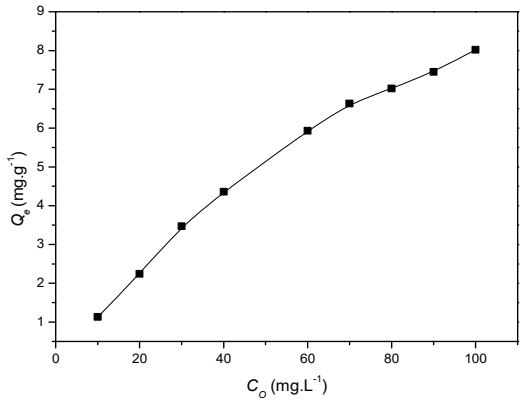

Figure10. Effect of initial concentration of MB on the maximum capacity of adsorption

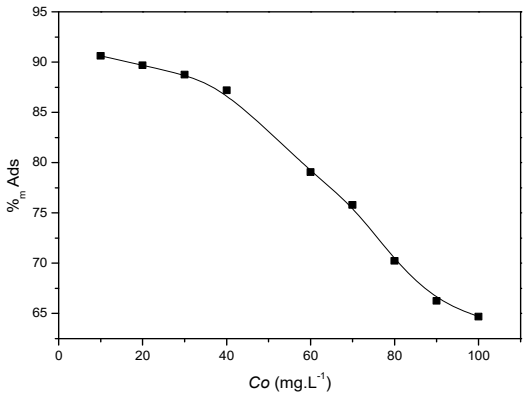

Figure11. Effect of initial concentration of MB on the maximum percentage of adsorption

Effect of pH

Table 3, Figures 12 and 13 present the results of the effect of the pH of the MB solution on the adsorption. From these results it appeared that the maximum adsorption capacity and maximum adsorption percentage increase with the pH of the

MB solution. The optimum maximum adsorption capacity and maximum adsorption percentage are evaluated at 8.86 mg/g and 88.67%, at pH 8.06, after 270 minutes.

Table 3. Maximum adsorption capacity (Q_m), maximum percentage of adsorption ($\%_m Ads$), and equilibrium time (t_e) at different pH

pH	Q_m(mg/g)	$\%_m Ads$	t_e(min)
2.04	5.19	51.19	270
4.09	5.38	53.38	300
6.61	5.38	86.13	190
8.06	8.86	88.63	270
10.04	9.01	90.13	240
12.08	9.31	93.13	300

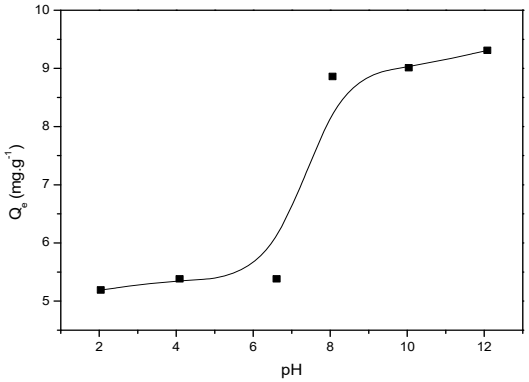

Figure 12. Effect of pH of MB solution on the maximum adsorption capacity of ECB

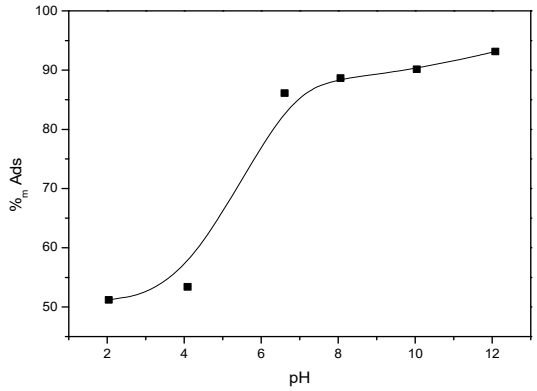

Figure13. Effect of pH of MB solution on the maximum percentage of adsorption of ECB

Modeling of adsorption kinetics

The results of the surface kinetic model presented in Table 4 show that the overall correlation coefficients (R^2_g)of the pseudo-first- order and the pseudo-second-order are respectively 0.8975 and 0.9002.

Table 4. Pseudo-first-order and pseudo-second-order parameters for the adsorption of MB onto ECB at different pH

pH	Pseudo-first-order parameters		Pseudo-second-order parameters	
	k_1(min^{-1})	R^2	k_2(gmg^{-1}min^{-1})	R^2
2.04	0.0089	0.9342	0.0122	0.8456
4.09	0.0076	0.9374	0.0088	0.8969
6.61	0.0148	0.8459	0.0254	0.9453
8.06	0.0124	0.9156	0.0274	0.8279
10.04	0.0119	0.8824	0.0122	0.9640
12.08	0.0082	0.8695	0.0078	0.9218
R^2g		0.8975	0.9002	

Modeling of adsorption isotherms

The results of modeling adsorption isotherms according to the Langmuir and Freundlich equilibrium models are given in Table 5. The specific parameters of each model have been determined, including Q_m, K_L and R_L (Langmuir parameters) and K_F and $1/n$ (Freundlich parameters).

DISCUSSION

The maximum observed adsorption capacity (Q_{mo}) of ECB with a value of 89.99 mg g^{-1} (Table 1) is very high compared to that reported by Rahimian and Zarinabadi (2020) with 40.0 mg g^{-1} for the leaves of pine trees bioadsorbent. The pH_{ZPC} of 5.51 indicates that the surface of the bioadsorbent is neutral at this pH, positive at a pH <pH_{ZPC} and negative at pH>pH_{ZPC}. The decrease in maximum adsorption capacity with increasing biosorbent mass is due to the biosorbent mass effect resulting from steric hindrance (Table 2 and Figure 2).This phenomenon makes some active sites of the biosorbent inaccessible, but taken into account in the calculation of the adsorption capacity (Kifuani *et al.,* 2018a). The increase in the maximum adsorption percentage with the mass of the biosorbent is due to the increase in the number of free active sites with the mass of the biosorbent (Table 2 and Figure 3). Similar observation was reported by Kifuani *et al.* (2018a) in studying the adsorption of methylene blue in aqueous solution on a biosorbent from agricultural waste of *Cucumeropsismannii* Naudin. Other authors also obtained similar results (Razia *et al.,* 2022). The increase in adsorption capacity or percentage of adsorption of ECB biosorbent with contact time is due to the availability of the number of free sites of adsorption, with are many at the beginning of adsorption and which gradually saturate with contact time. This explains the three phases of the curves (Figures 4 to 9). The horizontal part of the curve shows a total saturation of adsorption sites, and indicates that the maximum apparent adsorption capacity is reached (Kifuani *et al.,* 2018a; Nigist *et al.,* 2022; Gani *et al.,* 2023; Ajala *et al.,* 2024). The increase of the adsorption capacity with the initial MB concentration is due to the increase in the availability of free sites with the increase of the concentration of the MB solution (Figures 10 and 11).

Table 5. Langmuir and Freundlich parameters for the adsorption of MB onto ECB at different pH

pH	Langmuir parameters					Freundlich parameters		
	Q_m calculated	Q_m (mg.g^{-1})	K_L	R_L	R^2	K_f^* (mg.g^{-1})(mgL^{-1})$^{-1/n}$	$1/n$	R^2
2.04	24.00	5.19	0.2157	0.0848	0.9185	2.4481	0.1928	0.9288
4.09	23.14	5.38	0.2324	0.0792	0.9683	0.1539	0.9085	0.9264
6.61	6.93	5.38	0.7763	0.0251	0.9051	1.1106	0.4054	0.7543
8.06	5.69	8.86	1.5571	0.0120	0.9973	0.4506	0.7614	0.9732
10.04	4.94	9.01	1.8239	0.0108	0.9784	2.8832	0.2909	0.9596
12.08	3.44	9.31	2.7064	0.0073	0.9531	0.5558	0.7206	0.9721
R^2g					0.9534	0.9191		

There is an increase in the diffusion of the solute particles with the increase in the mass of the solute according to Fick's law. On the other hand, the maximum adsorption percentage decreases with the increase in the MB concentration because of the increase in the agglomeration of the solute particles with the initial concentration. Musah *et al.* (2020) also reported the same observations on the decrease in the adsorption percentage with the concentration of the solution for the adsorption of methylene blue on a biosorbent from *Platanus orientalis* leaf powder.

The pH determines the surface charge of the biosorbent, which depends on the pH_{ZPC}. The distribution of charges on the surface (S) of the biosorbent is as follows:

At pH <pH_{ZPC}: S-OH + H_3O^+ ↔ SO^+H_2 + H_2O
At pH= pH_{ZPC}: SO^+H_2↔ S-OH + H^+
At pH>pH_{ZPC}:S-OH + HO^- ↔ $S\text{-}O^-$ + H_2O

At pH= pH_{ZPC} (=5.51), the surface of the biosorbent is neutral. Below the pH_{ZPC}, the surface of the biosorbent is positively charged, hence the decrease in adsorption observed due to repulsive interactions between the surface of the biosorbent and the organic ions of MB. Beyond the $pH_{ZPC,}$ the surface of the biosorbent is negatively charged, there are then attractive interactions between the surface of the biosorbent and the organic cations, which lead to an increase in the capacity and the percentage of adsorption (Table 3, Figures 12 and 13). The optimum pH was estimated to be 8.06 with an optimum Q_m of 8.86 mg/g and optimum $\%_m Ads$ of 88.63%. Similar results were obtained by other authors with different adsorbents (Mekhalef *et al.,* 2018, Gajendiran *et al.,* 2024). The overall correlation coefficients of the pseudo-first-order and pseudo-second-order kinetic models are practically very similar, both models are therefore suitable for describing the adsorption of MB on ECB (Table 4).However, the pseudo-second-order kinetic model is better suited to describe the adsorption of MB on ECB biosorbent. This correlation assumes that adsorption is governed by the attachment of MB particles to the surface of the biosorbent (Kifuani, 2013). This correlation, less than 1, does not exclude other adsorption mechanisms. Similar kinetic results have been reported in the literature (Musah *et al.,* 2020). The adsorption isotherm modelling results show that the Langmuir model (R^2_g=0.9534) is better suited to describe the adsorption of MB on ECB compared to the Freundlich model (R^2_g=0.9191)(Table 5). This correlation with Langmuir model indicates monolayer adsorption on the surface of the biosorbent (Narayana and Ravi, 2019). The equilibrium parameter or separation parameter, K_L, indicates the affinity of the biosorbent towards methylene blue, which can be favorable (0 <R_L<1), irreversible (R_L=0), linear (R_L =1) or unfavorable (R_L>1) (Thiene *et al.,* 2024). The K_F values represent the adsorbent power of the biosorbent, when the concentration (C_e) of MB is unitary. The Freundlich parameter 1/*n* indicate the adsorption intensity or adsorption interaction strength. It is reported that the adsorption can be favorable (1/*n*<1), linear (1/*n* = 1), physical and unfavorable (1/*n*>1) (Bharath *et al.,* 2022; Basma *et al.* 2024;Hajir *et al.* 2024).The values of $R_L$and 1/*n*less than 1 obtained for all pH studied, indicate that the adsorption of MB on ECB biosorbent is favorable.

Conclusion

The biosorbent based on water hyacinth stems and leaves were used for the removal of MB organic dye in aqueous solution. Adsorption were carried out in batch tests bye varying several parameters. The obtained results show that the ECB biosorbent has a specific surface area of 296.52 m^2 g^{-1} and a maximum observed adsorption capacity (Q_{mo}) of 89.99 mg g^{-1}. The maximum adsorption capacity and the maximum percentage of the ECB biosorbent increase with the MB-ECB contact time and the pH of the MB solution. The adsorption of MB on ECB biosorbent is better in basic medium. The maximum adsorption percentage increases with the mass of the biosorbent. This increase is due to the availability of a large number of free sites with the increasing mass of the biosorbent. The optimal condition determined are 800 mg of MB at a pH of 8.06 with an adsorption percentage of adsorption of 88.63% after 270 minutes. Adsorption kinetics and equilibrium modeling showed that the adsorption of MB on ECB is best described by the pseudo-second order kinetic model and the Langmuir model. The values of $R_L$and 1/*n* less than 1 obtained for all pH studied, indicate that the adsorption of MB on ECB biosorbent is favorable. The results obtained in this study show that water hyacinth is effective for removal organic dyes from water.

Competing interests: The authors declare that they have no competing interests.

Authors' contributions: All authors contributed to data analysis and discussion of results.

Acknowledgements: The authors of the manuscript gratefully acknowledge Jerry IKELE KURAYUM and Kifline MILEBUDI KIFUANI family for the facilities provided to Professor Anatole KIA MAYEKO KIFUANI, during the final editing of this article in Aurora-Denver, Colorado, USA.

REFERENCES

Ajala, E.O., Aliyu, M.O., Ajala, M.A., Mamba, G., Ndana, A.M., Olatunde, and T.S. 2024. Adsorption of lead and chromium ions from electroplating wastewater using plantain stalk modified by amorphous alumina developed from waste cans. *Scientific reports*, 14:6055. DOI: https://doi.org/10.1038/s41598-024-56183-2.

Ali, K., Javaid, U.J., Ali, Z., and Zaghum, M.J. 2021. Biomass-derived adsorbents for dye and heavy metal removal from wastewater. *Adsorption Science and Technology*, 2021:1-14. DOI: https://doi.org/10.1155/2021/9357509.

Alouani, M.EL., Alehyen, S., Achouri, M.EL., and Taibi, M. 2018. Removal of cationic dye methylene blue from aqueous soution by adsorption on fly ash-based geoplymer. *J. Mater. Envir. Sci.,* 9(1):32-46. DOI: https://dx.doi.org/10.26872/jmes.2018.9.1.5.

Basma, G., and Alhogbi, G. S. A. 2023. An investigation of a natural biosorbent for removing methylene blue dye from aqueous solution. Molecules, 28 (6) : 2785. DOI: https://doi.org/10.3390/molecules 28062785.

Basma, I.W., Israa, S.AB., Asrar, A.A., and Marial, A.M. 2024. Adsorption isotherms and kinetics studies of lead on polyacrylonitrile-based activated carbon nonwoven nanofibers. Ecological Engineering and Environmental Technology, 25 (6): 20-26. DOI: https: // doi.org/10.12912/27197050/186546.

Bharath, B.G., and Senthil, P. 2022. Adsorptive Removal of Alizarin Red S onto sulfuric acid modified avocado Seeds: Kinetics, Equilibrium, and Thermodynamic studies. Adsorption Science &Technology, 2022:ID3137870. DOI: https://doi.org/10.1155/2022/3137870.

Gani, P., andPuji, L. 2023. Comparison of two biosorbent beads for methylene blue discoloration in water. *J. Ecol. Eng.,* 24(8):137-145. DOI: https://doi.org/10.12911/22998993/166319.

Gajendiran, V., Deivasigamani, P., Sivamani, S., and Banarjee, S. 2024. Biochar from Manihot esculenta stalk as potential adsorbent for removal of reactive yellow dye. Desalination and water Treatment, 317: 100120. DOI: https://doi.org/10.1016/j.dwt.2024.100120.

Hajir, N., Abdelrahman, B.F., and Omar, A.S. 2024. Isothermal and kinetics investigation of dibenzothiophene removal from model fuel by activated carbon developed from mixed date seed and PET Wastes. *Journal of Ecological Engineering,* 25(3): 38–52. DOI: https://doi.org/10.12911/22998993/177628.

Hatiya, N.A., Reshad, A.S., and Negie, Z.W. 2022. Chemical modification of Neem (Azadirachta indica) biomass as bioadsorbent for removal of Pb2+ ion from aqueous wastewater. *Adsorption Science and Technology,* 2022 :1-18. DOI: https://doi.org/10.1155/2022/7813513.

Imran, M.S., Javed, T., Areej, I., and Haider, M.N. 2022. Sequestration of crystal violet dye from wastewater using low-cost coconut hust as a potential adsorbent. *Water. Sci. Technol,* 285 (8): 2295-2317. https://doi.org/10.2166/wst.2022.124

Jan, S.U., Ahmad, Y., Ali, M., Hussain, Z., and Melhi, S. 2022. Adsorptive removal of methylene blue from aqueous solution using sawdust. *Medicom Pharmaceutical Sciences,* 2 (1) : 8-16.

Jia, P., Tan, H., Liu, K., and Gao, W. 2018. Removal of methylene blue from aqueous solution by bone char. *Appl. Sci.,* 1903 :1-11. DOI : 10.3390/app8101903.

Kifuani, A.K.M., Noki, P.V., Ndelo, J.D.P., Mukana, W.M., Ekoko, G.B., Ilnga, B.L., and Mukinayi, J.M. 2012. Adsorption de la quinine bichlorhydrate sur charbon actif peu couteux à base de la bagasse de canne à sucre imprégnée de l'acide phosphorique. *Int. J. Biol. Chem. Sci.,* 6(3): 1337-1359. DOI: https: //dx.doi.org/10.4314/ijbcs.v6i3.36.

Kifuani, A.K.M. 2013. Adsorption des composés organiques aromatiques en solution aqueuse sur charbon actif à base des déchets agroindustriels. Thèse de doctorat, Université de Kinshasa.

Kifuani, K.M., Kifuani A.K.M., Ilinga, B.L., Ngoy, P.B., Monama, T.O., Ekoko, G.B., Mbala, B.M., and Muswema, J.L. 2018a. Adsorption d'un colorant basique Bleu de Methylene en solution aqueuse sur un bioadsorbant issu de dechets agricoles de Cucumeropsismannii Naudin. *Ind . J. Biol. Chem. Sci.,* 12 (1):558-575. DOI: https: //dx.doi.org/10.4314/ijbcs.v12i1.43.

Kifuani, K.M., Kifuani, A.K.M., Ilinga, B.L., Ngoy, P.B., Monama, T.O., Ekoko, G.B., and Muswema JL. 2018b. Kinetics and thermodynamic studies adsorption of Methylene Bleu in aqueous solution on a bioadsorbent from Cucumeropsismannii Naudin waste seeds. *Ind . J. Biol. Chem. Sci.,* 12 (5): 2412-2423. DOI: https://dx.doi.org/10.4314/ijbcs.v12i5.38.

Le, P.T., Bui, H.T., Le, T.H., Nguyen, T.H., Pham, L.A., Nguyen, H.N., Nguyen, Q.S., Nguyen, T.P., Bich, N.T., Duong, T.T., Herrmann, M., Ouillon, and Le T.P.Q. 2021. Preparation and characterization of biochar derived from agricultural by-products for dye removal. *Adsorption Science and Technology,* 2021: 1-21. DOI: https://doi.org/10.1155/2021/9161904.

Maryam, K., Nahid, G., Babak, M., and Mohsen, R. 2013. Removal of Methylene Blue from wastewater by adsorption onto ZnCl2 activated Corn Husk carbon : Equilibrium Studies. *Journal of Chemistry,* 2013 :1-6. DOI: http://dx.doi.org/10.1155/2013/383985.)

Mekhalef, B.F., Kacha, S.L.A., and Belaid, K.D. 2018. Étude comparative de l'adsorption du colorant Victoria Bleu Basique à partir de solutions aqueuses sur du carton usagé et de la sciure de bois. Revue des sciences de l'eau / *Journal of Water Science,* 31(2): 109–126. DOI: https://doi.org/10.7202/1051695ar.

Mekky, A.E.M., El-Masry, M.M., Khalifa, R.E., Omer, A.M., Tamer, T.M., Khan, Z.A., Gouda, M., Mohy,and Eldin M.S. 2020. Removal of methylene blue dye from synthetic aqueous solutions using dimethylglyoxime modified amberlite IRA-420: kinetic, equilibrium and thermodynamic studies. Desalination and Water Treatment, 181 : 399-411. DOI : 10.5004/dwt.2020.25097.

Merbouh, Ch., Belhsaien, K., Zouahri, A., and Iounes, N. 2020. Evaluation de la qualité physico-chimique des eaux souterraines au voisinage de la décharge contrôlée Mohammedia-Benslimane: Étude préliminaire. *European Scientific Journal,* 16(6). DOI : http://dx.doi.org/10.19044/esj.2020.v16n6p455.)

Mobalaji, M.J., Olatunde, S.D., Joshua, N.and E. 2021. Sequestration of hazardous dyes from aqueous solution using raw and modified agricultural waste. *Adsorption Science and Technology,* 2021 :1-21. DOI: https://doi.org/10.1155/2021/6297451.

Musah, B.M., Peng, L., and Xu, Y. 2020. Adsorption of methylene blue using chemically enhanced Platanus orientalis leaf powder : kinetics and mechanisms. *Nat. Env. &Poll. Tech.,* 19 (1) : 29-40. www.neptjournal.com.

Nadew, T.T., Keana, M., Sisay, T., Getye, B., and Habtu, N.G. 2023. Synthesis of activated carbon from banana peels for dye removal of an aqueous solution in textile industries: optimization, kinetics, and isotherm aspects. *Water Practice and Technology,* 18(4): 947-966. DOI: https://doi.org/10. 2166./wpt.2023.042

Narayana, S.K.V., and Ravi, V.K.. 2019. Adsorption isotherm studies on methylene blue dye removal using naturally available biosorbent. *Rasayan J. Chem.,* 12(4): 2176-2182. DOI :http://dx.doi.org/10.31788/RJC.2019.1245478.

Nigist, A.H., Ali, S.R., and Zemene, W.N. 2022. Chemical modification of neem (Azadirachta indica) biomass as bioadsorbent for removal of Pb2+ ion from aqueous wastewater. *Adsorption Science & Technology,* 2022: 18. DOI :https://doi.org/10.1155/2022/7813513.

Nyakairu, G.W.A., Kapanga, P.M., Ntale,M., Lusamba, S.N., Tshimanga, R.M., Ammari, A., and Shehu, Z. 2024. Synthesis, characterization and application of Zeolite/Bi2O3 nanocomposite in removal of Rhodamine B dye from wastewater. Cleaner Water, 1(2024) :100004. DOI: https : //dx.doi.org/10.1016/j.clwat.2024.100004.

Pathania, D., Sharma, S., and Singh, P. 2017. Removal of methylene blue by adsorption onto activated carbon developed from Ficus carica bast. *Arabian journal of chemistry,* 10: S1445-S1451. DOI: https: //dx.doi.org/10.1016/j.arabjc.2013.04.021.

Rahimian, R., and Zarinabadi, S. 2020. A review of studies on the removal of methylene blue dye from industrial wastewater using activated carbon adsorbents made from Almond Bark. *Prog. Biochem. Res.,* 3(3) : 251-268. DOI : 10.33945/PCBR.2020.3.8.

Raiyyaan, G.D., Khalith, M. S.B., Sheriff, A.M., and Arunachalam, K.D.A. 2021. Bio-adsorption of methylene

blue dye using chitosan-extracted from Fenneropenaeus indicus shrimp shell waste, *J. Aquac. Mar. Biol.,* 10 (4) : 146-150. https://medcraveonline.com.

Razia, S., Syed, N.T., Usman, T.S., Yunus, K.T.M., Shaik, D.A.K., Imran, M., Kiran, S.M. A., Kalam, M.A., Ananda, M,H.C., and Akheel, AS. 2022, Adsorption of Crystal Violet dye from aqueous solution using industrial pepper seed spent: Equilibrium, *Thermodynamic, and Kinetic Studies. Adsorption Science & Technology.,* 2022:ID9009 214. DOI:https://doi.org/10.1155/2022/9009214.

Saad, T.M., Salah, O.H., Hussein, T.K., Ahjel, S., Abas, R.R., Alzahraa, Z.H., Muften, N.F.M., and Omram, A.A. 2024. Grass waste: A highly biosorbent for the removal of malachite green dye from aqueous solution. *Arabian Journal of Green Chemistry,* 8 (3): 349-359. DOI: 10. 48309/AJGC.2024.449167.1489.

Tshiene, B.W., Kifuani, K.M., Kifuani, A.K.M., Ngoy, P.B., and Ekoko, G.B., Adsorption of a basic dye methylene blue in aqueous solution on a bioadsorbent from agricultural waste of Manihot esculenta Crantz. 2024. *Int, J. Biol. Chem. Sci.,* 18 (3): 1180-1198. DOI: https://dx.doi.org/ 10.4314/ijbcs.v 18i3.35.

Vanessa, P. V., Andrin A., Le ,B. M., Lacombe, S., Frayret, J., and Pigot, T. 2017. Couplage photocatalytique-oxydation par le ferrate-VI pour le traitement du colorant Rhodamine 6G. Revue des Sciences de l'eau, 30(1):35-39. DOI: https : //dx.doi.org/10.7202/104006Lar.

****